1 Electrodynamics of solids — Introduction to practicum

Contents

In this introduction, some of the theoretical approaches used in the analysis of optical spectra of solids are briefly summarized. For more details, readers are encouraged to consults the following books, see Refs. [1–3].

1.1 Dielectric function

The goal of the optical spectroscopy is to determine the real and imaginary part of the dielectric function $\varepsilon(\omega) = \varepsilon_1(\omega) + \mathrm{i}\varepsilon_2(\omega)$ that is defined as a ratio of the polarization (volume density of the electric dipoles) P and the average total electric field E

$$\varepsilon(\omega) = 1 + \frac{P(\omega)}{\varepsilon_0 E(\omega)} \,, \tag{1}$$

where $P(\omega)$ and $E(\omega)$ are the Fourier coefficients of the corresponding time dependent quantities. Dielectric function is connected to the index of refraction as $N(\omega) = \sqrt{\varepsilon(\omega)}$. It is often useful, particularly for conducting materials, to express the optical constants in terms of the optical conductivity $\sigma(\omega) = -\mathrm{i}\omega\epsilon_0(\varepsilon(\omega) - 1)$, where ϵ_0 is the permittivity of vacuum. The real part of the optical conductivity $\sigma_1(\omega)$ represents the absorption of electromagnetic radiation per unit of frequency and at zero frequency it yields the DC conductivity.

1.2 Fresnel coefficients

Consider an electromagnetic wave incident from a material with index of refraction N_i on a planar interface with another material with the index of refraction N_t. The ratio of the electric field of reflected wave (r) or transmitted wave (t) with respect to the incident wave is given by the so-called Fresnel coefficients. In case of isotropic materials, the coefficients read

$$r_\mathrm{s} = \frac{N_i \cos\theta_i - N_t \cos\theta_t}{N_i \cos\theta_i + N_t \cos\theta_t} \,, \quad r_\mathrm{p} = \frac{N_t \cos\theta_i - N_i \cos\theta_t}{N_t \cos\theta_i + N_i \cos\theta_t} \,, \tag{2}$$

$$t_{\rm s} = \frac{2N_i\cos\theta_i}{N_i\cos\theta_i + N_t\cos\theta_t}\ , \quad t_{\rm p} = \frac{2N_i\cos\theta_i - N_i\cos\theta_t}{N_t\cos\theta_i + N_i\cos\theta_t}\ , \tag{3}$$

where θ_i and θ_t are the angles of the incident and transmitted wave with respect to normal. The indexes 's' and 'p' denote the wave with perpendicular and parallel electric vector with respect to the plane of incidence. In case of the near normal incidence reflectivity (the case often used in experiments) the expressions (2) simplify to

$$r = \frac{1-N_t}{1+N_t}\ . \tag{4}$$

The latter formula holds for a semi infinite sample, i.e., a sample that is either thicker then the penetration depth or with roughened back side so that the back side reflected wave does not reach the detector. In reflection experiment, we measure the ratio of intensities of radiation $R = |r|^2$. The intensity of the incident radiation is measured using a reference sample. In infrared range, a golden coated sample is typically used since gold has an almost spectrally independent reflectivity of about 0.98%.

In case of an anisotropic medium with orthorhombic symmetry, the dielectric function is a tensor with three diagonal components ε_x, ε_y and ε_z corresponding to the dielectric functions along the x, y and z axis respectively. In this case, the Fresnel reflection coefficients read

$$r_{\rm s} = \frac{N_i\cos\theta_i - \sqrt{N_{ty}^2 - N_i^2\sin^2\theta_i}}{N_i\cos\theta_i + \sqrt{N_{ty}^2 - N_i^2\sin^2\theta_i}}\ , \quad r_{\rm p} = \frac{N_{tx}N_{tz}\cos\theta_i - N_i\sqrt{N_{tz}^2 - N_i^2\sin^2\theta_i}}{N_{tx}N_{tz}\cos\theta_i + N_i\sqrt{N_{tz}^2 - N_i^2\sin^2\theta_i}}\ , \tag{5}$$

where N_{tx}, N_{ty}, N_{tz} is the index of refraction along the x, y and z axis respectively. For a thorough discussion of a propagation of light in the anisotropic media, see, e.g., Ref. [1].

1.3 Models of the dielectric function

We shell consider several models of the dielectric function that might be usefull in analysis of data since

- they help to get an insight into the processes responsible for the polarization
- they are Kramers-Kronig consistent, which might not be necessarily true for the data obtained point by point. Analysis using Kramers-Kronig consistent dielectric function may allow to determine other unknown parameters of the system, e.g., thicknesses of the layers (including surface roughness), more components of the dielectric tensor of anisotropic material etc.
- they represent the point-by-point data by small set of parameters.

Below we summarize most frequent models. Since the dielectric function is additive, any combination of these models can be considered.

1.3.1 Lorentz model

The Lorentz model is derived from the response of harmonic oscillators with density n, mass m and charge Q. The contribution of a single Lorentz oscillator to the dielectric function can be expressed as

$$\varepsilon(\omega) = \frac{\omega_{\rm pl}^2}{\omega_0^2 - \omega^2 - {\rm i}\omega\gamma}\ , \tag{6}$$

The Lorentz oscillator has thus three parameters: the center frequency ω_0, the plasma frequency $\omega_{\rm pl}$ and broadening γ. It can be shown that $\omega_{\rm pl} = \sqrt{nQ^2/\epsilon_0 m}$. Since the model is derived from Newton equations, it is inherently Kramers-Kronig consistent. The real and imaginary part of the dielectric function of one Lorentz oscillator is shown in Fig. 1.

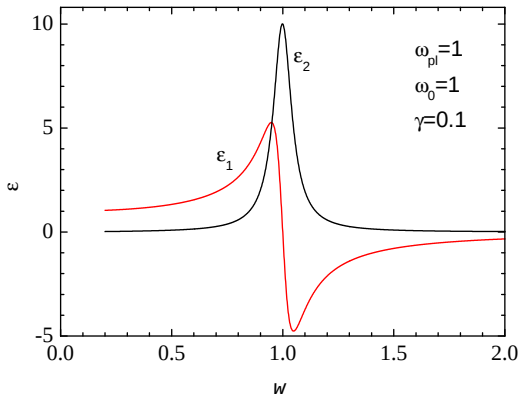

Figure 1: The real and imaginary part of a Lorentz oscillator.

In a more general case, there can be several Lorentz oscillators and the total dielectric function is then given by the sum

$$\varepsilon = \epsilon_\infty + \sum_k \frac{\omega_{\mathrm{pl},k}^2}{\omega_k^2 - \omega^2 - \mathrm{i}\omega\gamma_k} \ . \tag{7}$$

The latter formula has in addition the real constant ϵ_∞, that can be viewed as a contribution of polarization processes at a higher frequency than the studied range. Indeed, the low frequency limit of the Lorentz oscillator (6) is a constant. However, this constant is only an approximation. Instead of a constant, a more accurate approach would be considering a Lorentz oscillator with zero broadening at a higher frequency than the studied range. This is the so called Sellmeier model discussed in more detail below.

The Lorentz model (7), despite its simplicity, is already a versatile model that can be used in a number of situations. It fits remarkably well the response of infrared active lattice vibrations.

1.3.2 Drude model

The response of free charge carriers, so called Drude model, is obtained as the limit of the Lorentz oscillator for zero restoring force, that is, for $\omega_0 = 0$

$$\varepsilon_{\mathrm{Drude}}(\omega) = -\frac{\omega_{\mathrm{pl}}^2}{\omega(\omega + \mathrm{i}\gamma)} \ . \tag{8}$$

The dielectric function $\varepsilon(\omega) = 1 + \varepsilon_{\mathrm{Drude}}(\omega)$ and the corresponding optical conductivity are shown in Fig. 2(a) and 2(b), respectively. Note that the $\varepsilon_2(\omega)$ diverges at zero frequency whereas the conductivity is finite and yields the DC conductivity.

This term usually represents well the frequency response of doped semiconductors or metals. In case there are multiple bands crossing the Fermi level, one Drude term should be used for each band. In case of correlated metals, e.g. high temperature superconductors, where the free charge carriers are interacting, the scattering rate $1/\gamma$ depends on frequency. This case can be on a phenomenological level modelled also using multiple Drude terms.

1.3.3 Sellmeier and Cauchy models

Sellmeier and Cauchy models are used to model the well known dispersion of optical constants in the transparent frequency range. The Selmaier model is obtained by considering Lorentz oscillators (one

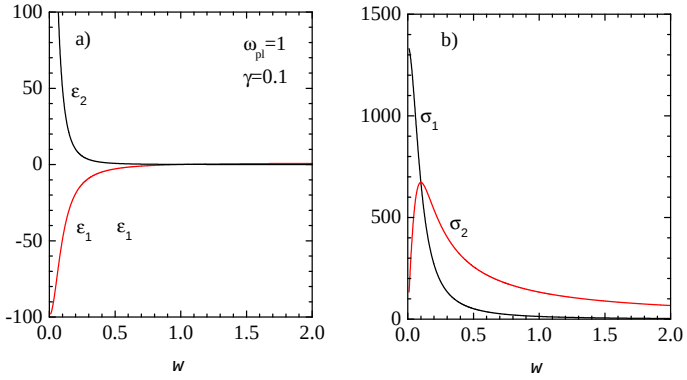

Figure 2: The real and imaginary part of the Drude model oscillators with values of parameters shown in the Figure.

or two are usually enough) at frequencies above the transparent region

$$\varepsilon(\omega) = \sum_k \frac{\omega_{\mathrm{pl},k}^2}{\omega_k^2 - \omega^2} \ . \tag{9}$$

In the simplest case with one oscillator, the model as only two parameters: the frequency and the plasma frequency.

The Cauchy model is a model for index of refraction obtained from an expansion of the Sellmeier model at zero frequency

$$N(\lambda) = A + \frac{B}{\lambda^2} + \frac{C}{\lambda^4} + \dots \ . \tag{10}$$

Here, the unknowns are the expansion constants A, B and C. Figure 3 shows the real part of the dielectric function of one Lorentz oscillator located at $\omega = 1$ and the Cauchy model fitted to the Sellmeier model up to $\omega = 0.7$. Some deviations between the two models can be noticed arising from the fact that the Cauchy model is only approximative.

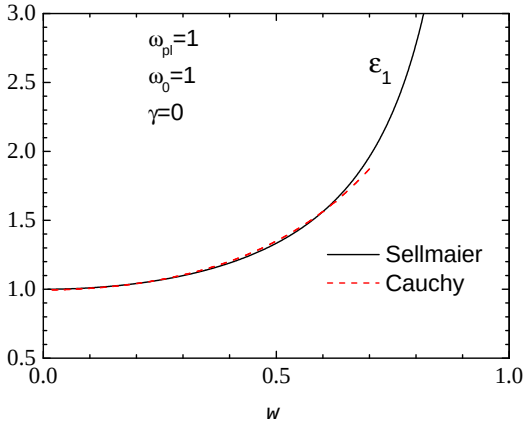

Figure 3: Sellmeier model with one Lorentzian with zero broadening located at $\omega = 1$ (solid line). Cauchy model (red dashed line) is fitted to the Sellmeier model up to $\omega = 0.7$.

1.3.4 Complex Lorentzian model

In the case the phonon modes are interacting (e.g. due to a nonparabolic potential), the phonon resonances have an asymmetric shape. This can be modelled using a generalized Lorentz oscillator with a complex plasma frequency [4]

$$\varepsilon(\omega) = \frac{\omega_{\mathrm{pl}}^2 + \mathrm{i}\omega\omega_c}{\omega_0^2 - \omega^2 - \mathrm{i}\omega\gamma} \ . \tag{11}$$

The complex nominator essentially mixes the real and imaginary part of the standard Lorentz oscillator so that an asymmetric shape is obtained. This model is often used e.g. for modeling of phonon response in perovskite oxides that often exhibit an asymmetric shape.

Figure 4 displays the complex Lorentzian profile for various values of ω_{pl} and ω_c in such a way that the absolute value of the nominator is approximately constant. In Fig. 4(a), it can be seen that, as the imaginary part ω_c increases, ε_2 gradually transforms to the negatively taken ε_1 of the Lorentz oscillator, and vice versa for the ε_1, see Fig. 4(b). The opposite trend is seen for negative values of ω_c, see Figs. 4(c) and (d).

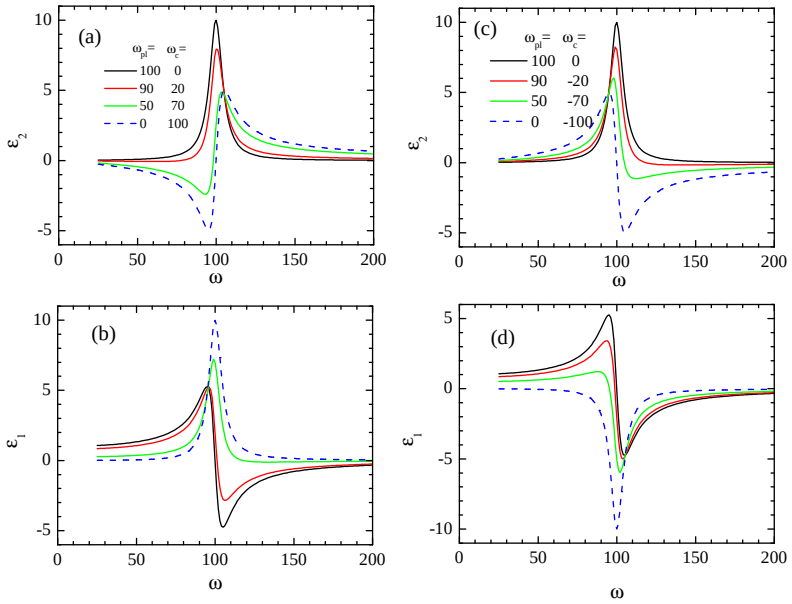

Figure 4: The complex Lorentzian model for various values of parameters shown in the panels (a) and (c).

1.3.5 Gaussian lineshape

In some cases, the lineshapes can have the Gaussian shape rather then the shape of a Lorenztian oscillator. For example, the center frequency might have a gaussian distribution due to a disorder. The ε_2 of the Gaussian lineshape reads

$$\varepsilon_2(\omega) = A\left(\varepsilon^{-\left(\frac{\omega-\omega_0}{\sigma}\right)^2} + \varepsilon^{-\left(\frac{\omega+\omega_0}{\sigma}\right)^2}\right) \ . \tag{12}$$

The two Gaussians centered at ω_0 and $-\omega_0$ are necessary so that the total dielectric function fulfills the Kramers-Kronig requirement $\varepsilon(\omega) = \varepsilon(-\omega)^*$. The imaginary part of the contribution to the dielectric function is then calculated numerically using the Kramers-Kronig relations.

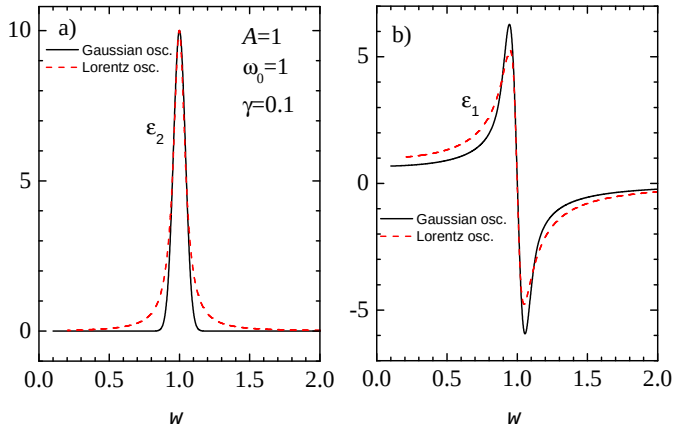

Figure 5: The imaginary (a) and real (b) part of the dielectric function of Gaussian lineshape compared to the Lorentzian lineshape with the same width at half maximum.

Compared to the Lorentzian function, see Fig. 5, the Gaussian lineshape has an exponential (and thus much faster) fall-off from the center frequency. In more general case, a convolution between Gauss and Lorentz lineshape, so called Voigt model, can be considered.

1.3.6 Tauc-Lorentz model

Tauc-Lorentz oscillator was developped by Jellison and Modine [5] for modeling of the dielectric function of amorphous materials. For $E > E_g$ the formula for ε_2 reads

$$\varepsilon_2(E) = \frac{AE_0C(E-E_g)^2}{(E^2-E_0^2)^2+C^2E^2}\frac{1}{E} \tag{13}$$

Below the bandgap, the absoprtion is zero. Close to the band edge E_g, the absorption follows the Tauc law formula, $\varepsilon_2(E) \propto (E-E_g)^2/E^2$. The ε_1 is calculated using Kramers-Kronig relations and can be analytically expressed, see Ref. [1, 5]. Figure 6 displays the dielectric function of the Tauc Lorentz model for selected values of parameters.

1.3.7 Critical point parabolic band

The critical points of interband transitions of crystallines solids are often analyzed with the critical point parabolic band model fitted usually to the second or third derivative of the dielectric function in order to suppress the background [6,7]. In this model, the contribution of a parabolic critical point (CP) located at an energy E_{CP} to the j-th derivative of the dielectric function reads

$$\frac{\mathrm{d}^j\varepsilon(E)}{\mathrm{d}E^j} = Ae^{\mathrm{i}\phi}(E-E_{\mathrm{CP}}+\mathrm{i}\Gamma)^{-n-j}\ , \tag{14}$$

where A and ϕ are amplitude and phase factor and n has the values -1/2, 0 and 1/2 for three-, two- and one-dimensional CP, respectively.

1.3.8 Bruggeman effective medium approximation and surface roughness

Effective medium approximations describe the effective optical properties of a composite material formed by a mixture of two or more components that are assumed to be homogeneously intermixed

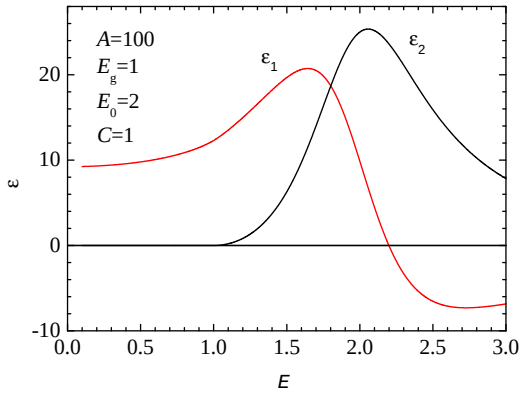

Figure 6: The real and imaginary part of the Tauc-Lorentz model for the values of parameters shown in the figure.

on a scale that is much smaller than the used wavelength of light. There are various approaches how to calculate the effective dielectric function. One of them is the Bruggeman formula that for circular inclusions in three dimensions reads

$$\sum_i \delta_i \frac{\varepsilon_i - \varepsilon_e}{\varepsilon_i + 2\varepsilon_e} = 0 \,. \tag{15}$$

The summation is effectuated over components indexed with i, with volume fractions δ_i and dielectric function ε_i. The effective dielectric function ε_e is obtained after solving the latter equation.

The Brugemman formula is used in order to calculate the influence of the surface roughness to optical measurements. Ellipsometry is particularly sensitive to the surface roughness. A roughness with magnitude of only few Angstroms gives rise to already noticeable effect on the ellipsometric angle Δ. In order to take this effect in to account, it is assumed that the surface roughness can be approximated by a layer composed of 50% by the material and of 50% by air or vacuum. Assuming a dielectric function of the material, the only free parameter to be determined is the thickness of the surface roughness layer. In the case there is a transparent region within the measurement range, the Sellmeier (or Cauchy) model can be used and the thickness of the surface roughness layer is determined together with the Sellmeier model parameters. In the case there is no absorbing region in the measurements range, e.g., in metals, this approach cannot be used. One possibility is to determine the surface roughness magnitude from the atomic force microscopy.

The interfacial roughness between two materials can be modelled in an analogous way.

1.4 Principles of ellipsometry

The ellipsometric measurements make use of the change of the polarization state of light after the reflection (or transmission) from sample. The simplest ellipsometric configuration with two polarizers is schematically depicted in Fig. 7. Light coming from the source is polarized by the first polarizer and is incident on the sample at an angle θ_i. Since the Fresnel reflection coefficient for s and p polarized component of the wave have generally different real and imaginary part, the amplitude and phase of the reflected s and p components differ. They interfere coherently and give rise to an elliptically polarized state which is analyzed by the second polarizer, the so-called analyzer. Typically, the intensity of light is measured as a function of the analyzer angle. This is the so-called rotating analyzer ellipsometry.

In the ellipsometric measurement, the obtained measured quantities are the ellipsometric angles

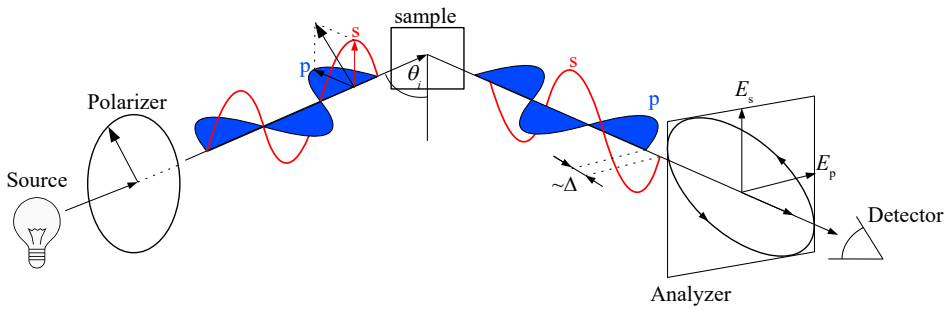

Figure 7: Scheme depicting the principle of ellipsometry.

Ψ and Δ defined using the complex quantity ρ as

$$\rho(\Psi,\Delta) = \operatorname{tg}\Psi e^{\mathrm{i}\Delta} = \frac{r_p}{r_s}\,. \tag{16}$$

It can be shown, that on a semi-infinite isotropic sample, the dielectric function of the sample ε_t can be expressed as a function of ρ as

$$\varepsilon_t(\Psi,\Delta) = \varepsilon_i \sin^2\theta_i \left(1 + \operatorname{tg}^2\theta_i \left(\frac{1-\rho(\Psi,\Delta)}{1+\rho(\Psi,\Delta)}\right)\right)\,. \tag{17}$$

The complex dielectric function ε_t with two unknown quantities (the real and the imaginary part) is obtained from two measured quantities, Ψ and Δ. In this most simple case, this relation is analytical. In more complicated cases (e.g. thin films on a substrate), the dielectric function cannot be obtained analytically and has to be obtained numerically using regression analysis, where the optical constants are sought in order that the theoretically calculated Ψ and Δ matches the experimentally measured values. However, even in the case of thin films, it is often instructive to look at the data using Eq. (17) since the resulting ε_t already does not depend on the angle of incidence in the trivial way as the ellipsometric angles Ψ and Δ do. However in this case it cannot be considered as the dielectric function, so it is called the pseudo-dielectric function.

In the rotating analyzer ellipsometry, the quantities that are determined are actually $\operatorname{tg}\Psi$ and $\cos\Delta$. Therefore the errorbar of Δ diverges as Δ approaches 0 and 180°. Mainly for this reason, advanced ellipsometric setups were developed that employ waveplates (so called compensators) that shift the phase betwen s and p polarized wave. A series of measuremets with different degrees of phase shifts are measured in the so-called rotating compensator ellipsometry. As a results Δ is precisely measured over the whole range 0-360°. In addition, depolarization can be determined. Depolarization arises when different polarization states interfere incoherently. Typically, it arises due to a finite frequency resolution of monochromator, lateral inhomogeneities either of the dielectric function or of film thickness; or due to reflections from the back side of the sample. These situations can be in principle modelled using Stokes vectors and Muller matrices that can handle partially polarized light [2].

1.4.1 Available spectroscopic equippment

The practicum tasks will be measured at nano core facility at CEITEC using Woollam VASE ellipsometer for near to ultraviolet range (0.5 to 6.5 eV) and Woollam IR-VASE ellipsometer for mid infrared range (300 to 6000 cm^{-1}). The far-infrared range (50 to 700 cm^{-1}) can be covered with near normal incidence reflection and transmission measurements using the vacuum Fourier transform spectrometer Bruker Vertex 70V.

The VASE ellipsometer is equipped with a double grating monochromator, photoconductive detector (Si/InGaAs) and a photomultiplier for high sensitivity in the UV range. It has a rotating compensator equivalent technology, the so called auto-retarder. The IR-VASE ellipsometer is a Fourier-transform spectrometer based ellipsometer equipped with a rotating compensator. Since both ellipsometers have rotating compensator, they can determine depolarization and Δ in the whole range 0-360°. In principle, they can measure 11 elements of the Muller matrix.

For analysis of the obtained data, the Woollam WVASE software can be employed.

1.5 Practicum tasks

1.5.1 Phonon spectra of isotropic and anisotropic semiconductors

1. Measure optical response of $SrTiO_3$ (isotropic crystal), GaN and SiO_2 (anisotropic crystals) in the frequency range of infrared active phonons. Use the polarized far-infrared reflection measurements complemented in mid-infrared range by ellipsometry.

2. Model the reflectivity and ellipsometry spectra by appropriate models and display the obtained dielectric function, and phonon parameter values.

1.5.2 Direct interband transitions in semiconductors

1. Measure the ellipsometric spectra of Si, GaN, CdS and InAs semiconductors.

2. Perform second derivative of the obtained pseudo-dielectric function and estimate the energy of the critical points.

3. Correct the data for the surface roughness and obtain a point-by point dielectric function of the materials.

4. Model the dielectric function of the materials with a suitable Kramers-Kronig consistent model.

1.5.3 Free charge carrier response in semiconductors and metals

1. Measure the ellispometric spectra of gold, doped Si, and a thin film of $La_{0.7}Sr_{0.3}CoO_3$ grown on LSAT substrate with VASE and IR-VASE ellipsometers.

2. Model the obtained spectra with appropriate models and determine the parameters of the Drude term. Estimate the concentration of charge carriers assuming tabulated value of the effective mass. Extrapolate the conductivity to zero frequency and compare it with tabulated DC conductivity values.

References

[1] H. Fujiwara, *Spectroscopic Ellipsometry, Principles and applications*, John Wiley & Sons Ltd, Chichester, 2007.

[2] *Handbook of Ellipsometry*, Tompkins, G. and Irene, E. edts. , A. William Andrew Publishing and Springer-Verlag GmbH & Co. KG, 2005.

[3] R. M. A. Azzam, N. M. Bashara, *Ellipsometry and Polarized Light*, North Holland; 3rd reprint 1999 edition, 1999.

[4] J. Humlíček, R. Henn, and M. Cardona, Phys. Rev. B **61**, 14 554 (2000).

[5] G. E. Jellison, Jr. and F. A. Modine, Appl. Phys. Lett. **69**, 371 (1996), Erratum, Appl. Phys. Lett. **69**, 2137 (1996).

[6] M. Cardona, Solid state physics, Modulation Spectroscopy, 1969.

[7] J. Humlíček and M. Garriga, Temperature Dependence of the Optical Spectra of $Si_{1-x}Ge_x$ Alloys, Silicon-Germanium Carbon Alloys Growth, Properties and Applications 483, 2002.